

Test Pattern Dependent Neural Network Systems for Guided Waves Damage Identification in Beams

C. K. LIEW, M. VEIDT
 Division of Mechanical Engineering
 University of Queensland
 Brisbane, Qld 4072
 AUSTRALIA

Abstract: - In regression neural networks for pattern recognition, a trained network may often produce large errors when identifying a test pattern not found in the training set. This is especially true when test patterns and training patterns are obtained from two different sources, as in the case from measured and simulated data. Therefore, this paper investigates a new neural network procedure where progressive training is performed in a series network with the implementation of a weight-range selection (WRS) technique that depends on the test pattern. An integer states rejection (ISR) criterion is also introduced to monitor and select the final network outputs. The WRS and ISR methods are applied for a supervised multi-layer perceptron operating with one hidden layer of neurons and trained using a backpropagation algorithm. An example of this system has been designed for damage identification in beams investigated with guided waves for structural health monitoring.

Key-Words: - pattern recognition, series network, generalization, ultrasonics, guided wave, damage evaluation

1 Introduction

Structural health monitoring is a field that aims to evaluate the integrity and safety of structures mainly for aerospace, civil and marine applications. The advent of advanced sensor technologies, accurate measuring instruments and the optimization in signal processing techniques [1] has motivated this area of research significantly to develop practical solutions to quantify damages in structures. One such technology that has gained much interest in the recent years is guided waves. Guided waves, an ultrasonics application, are highly sensitive in detecting discontinuities in its path of propagation [2]. However, identifying damages from the measured transient wave response alone can prove difficult when a reasonably large damage parameter space is considered. Signal processing thus becomes an essential intermediate procedure in guided waves damage identification, leading to the application of pattern recognition with neural networks.

Pattern recognition with regression neural networks has been recently developed for guided waves signals to quantify damages in beams [3] and in plates [4]. These systems require the simulation of patterns with known damage parameters for the supervised neural network training. Simulations of wave responses from the given damage parameters can be derived from considerations of the reflection and transmission coefficients at the damage boundaries [5] or by finite-element methods [6].

Although these simulations predict the wave response with adequate accuracy, there are some areas where experimental measurements can differ by small extents. These minor differences are sufficient to cause networks trained with simulated patterns to encounter difficulties in identifying experimental patterns. Examples of discrepancies can originate from noise, pulse interference, mode coupling, dispersion and additional wave modes, all of which are difficult to predict and hence, not easy to reproduce in simulation. The occurrences of most of these effects are case-specific, thus motivating the research of neural network training that depends on the test pattern being identified.

2 Weight-Range Selection (WRS) via a Series Network

The concept of a test pattern dependent neural network is possible by joining a few neural networks in series. The test outcome from a neural network can then be used to limit the parameter space for training the subsequent network. The weight-range selection (WRS) is proposed to fulfill this purpose to bridge between the networks in series.

2.1 Methodology

The initial iteration, I_0 , of the neural network is supervised through a training set of input-target pairs and if necessary, may include regularization or

validation with early stopping [7]. The trained network is then used to identify the test pattern. The test result is taken only as a sample, as it does not constitute a conclusive generalization of the network due to the random initialization of weights.

The random initialization of weights is a property of neural networks that results in no unique solution [8]. Training only ensures that for any random initial weights, the function approximated at the end of training gives minimum error with respect to the training set. Even when minimum error is achieved after training for a particular set of initial weights, the trained network might not necessarily give good generalization for the test pattern being identified. It is essential then to conduct a reasonable number of trials for training different random initial weights to obtain a quantitative measure of the quality of generalization. Identifying the test pattern can then be based on outputs averaged over all the trained neural networks from the trials. The content of the training set can also influence the neural network outputs, which have led to research in network ensembles applying methods like bagging and boosting [9]. These methods can complement WRS and is a subject of further research. In WRS, the training patterns are maintained when collecting samples from random initial weights but are changed in the next iteration when the training range size is reduced.

The WRS technique reduces the size of the output parameter space by statistical analysis of the sample results from the trials. Training data for the next neural processing in the series is then selected randomly within the new parameter space. Since the number of training patterns is to be kept constant throughout the series network, the WRS technique is only suitable for neural network problems with the availability of large data sets or data generation. Subsequently, initial weights are restricted to only those that allow the trained network to produce test pattern identification results within the parameter space. Results that fall outside the parameter space are from extrapolation, which are generally unreliable [10]. This procedure thus filters out poor initial weights and removes the unreliable results they produce from being considered as a sample.

Collecting a specified number of samples, K , marks the end of the iteration of a network in the series. The samples are then used in the next iteration for statistical analysis, and the cycle repeats until the maximum number of iterations, I_{max} , is achieved or other termination conditions are fulfilled. A flowchart describing the application of the WRS technique in a series network is illustrated in Figure 1. This flowchart accommodates training

with validation where validation patterns are also obtained within the training range. The statistical analysis of the samples is detailed in the next subsection while a termination point by a rejection threshold, seen in the figure, originates from a final outputs selection criterion described in section 3. Regardless of the termination point, the final outputs via WRS are the product of learning from a training set that is determined from results for the test pattern that is being identified in the first place. This creates a case-specific neural network that uniquely identifies only the test pattern that it depends on, naturally turning into a symbiotic system.

The rationale of reducing the size of the training range within the statistical boundaries of the test pattern identification results lies in the likelihood of improving generalization, which can be described by underfitting and overfitting [7]. Underfitting can be minimized, as the function approximated by the neural network for smaller parameter spaces is less complicated without the need to consider trends of patterns outside the space, thus promoting greater accuracy. Overfitting can also be minimized because in a smaller parameter space with the same number of patterns, the amount of interpolations required for regression can be reduced. However, it is important to note that ultimately, the quality of generalization depends on the mapping between inputs and targets, and the sensitivity of that mapping with respect to the test patterns.

2.2 Statistical Analysis

The statistical analysis performed on K samples of output results, O , extracts the mean output, $\langle O \rangle$, and the standard deviation, σ . These statistical properties are used to calculate the limits of the training range for data generation, $[ll, ul]$, and the limits of the range to accept O , $[LL, UL]$. Two types of limits are required because $[ll, ul]$ is not equal to $[LL, UL]$ when the actual solution is located close to the boundaries of the parameter space. In these cases, LL or UL is then allowed to fall outside the current parameter space to sustain a balanced spread of the sample results for the correct calculation of the mean. Extrapolation in this case is thus permitted and the results produced outside the training range are considered reliable.

The expressions and conditions that govern both limits for the i th iteration are given in Equations 1 and 2. n is a constant that denotes the number of standard deviations.

$$[LL_i, UL_i] = [\langle O \rangle_i - n\sigma_i, \langle O \rangle_i + n\sigma_i] ; i \neq 0 \tag{1}$$

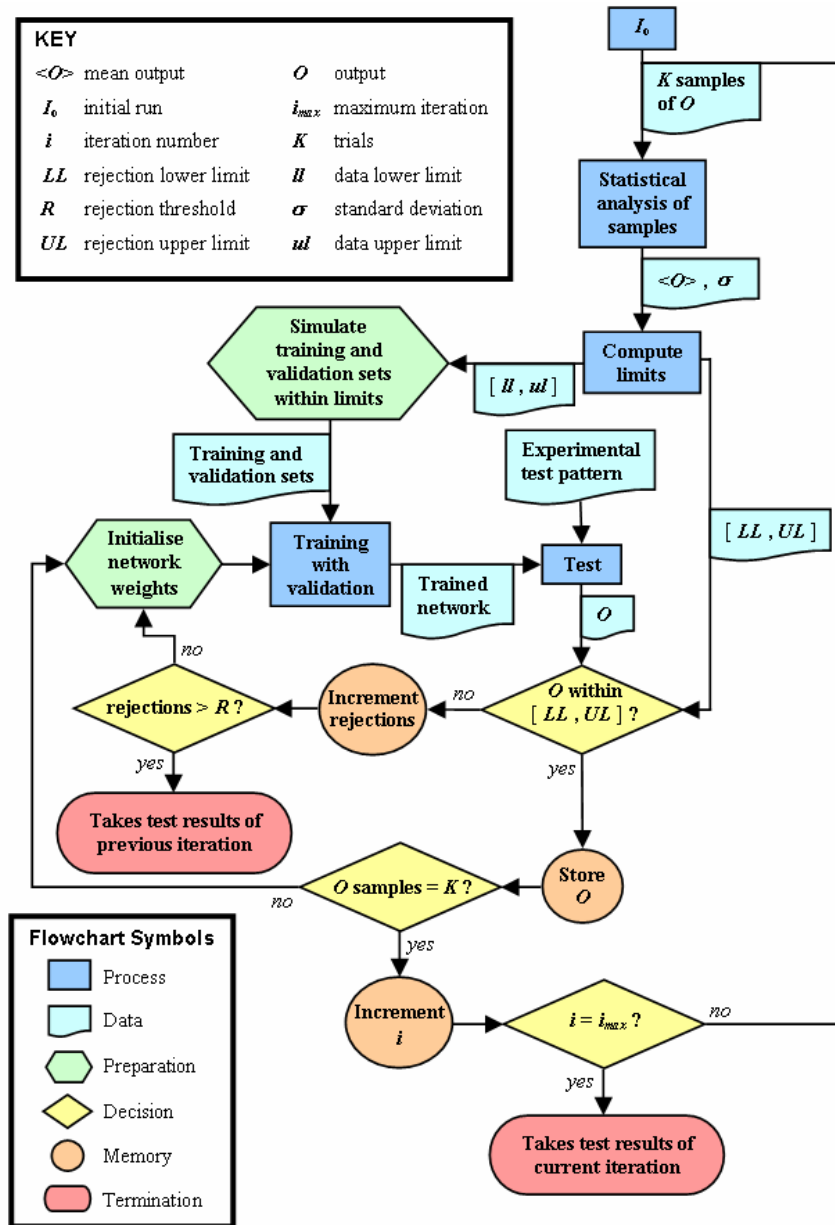


Fig. 1 Flowchart shows the process of the weight-range selection (WRS) technique in a series network.

$$[ll_i, ul_i] = \begin{cases} [ll_0, ul_0] & ; i = 0 \text{ OR} \\ & (LL_i < ll_0 \text{ AND } UL_i > ul_0) \\ [LL_i, ul_0] & ; i \neq 0 \text{ AND} \\ & LL_i > ll_0 \text{ AND } UL_i > ul_0 \\ [ll_0, UL_i] & ; i \neq 0 \text{ AND} \\ & LL_i < ll_0 \text{ AND } UL_i < ul_0 \\ [LL_i, UL_i] & ; i \neq 0 \text{ AND} \\ & LL_i > ll_0 \text{ AND } UL_i < ul_0 \end{cases} \quad (2)$$

Selection of n in Equation 1 can be based on sample distribution of past results for known output parameters of similar neural network tests or the

confidence level desired for the new range. More confident ranges can be achieved by choosing a larger n value. However, n is inversely related to the range reduction rate and it is thus not recommended to go beyond 2σ 's, otherwise the range converges too slowly to the parameters identified, causing the need for many iterations of the series network and an impractically long processing time.

Equation 1 shows the application of simple statistical calculations to determine the limits of the new parameter space while reducing the size of the training range. This equation can be modified or replaced with more favourable expressions based on statistics or other mathematical concepts that can better represent the distribution of the samples.

3 Integer States Rejection (ISR)

Criterion

With the application of Equation 1, the parameter space reduces in size with iterations in the series network. When the parameter space becomes too small, it is possible for the actual solution to fall outside the training range. Pattern recognition in subsequent networks in the series then becomes an extrapolation and this may cause poor generalization in the neural network. A proposed approach to prevent such occurrences is the integer states rejection (ISR) criterion.

Integer state is a term adopted from MATLAB[®], which is used by its random number generator [11] to initialize all the weights in the network. These integer states provide an efficient way to track and reproduce the network weights for consistent evaluation of neural network performance. The ISR criterion takes advantage of this property to monitor the number of rejected samples. A sample is rejected when network weights initialized by an integer state are trained and yield output results that fall outside the accepted range, $[LL, UL]$, of the current network iteration. Integer states that produce accepted samples can be stored and be used to repeat a good training run.

The ISR criterion can also be useful in stopping the iterative process of the series network and in selecting the final output predictions. A rejection threshold, R , can be set to achieve this, as shown in Figure 1. If the number of rejections exceeds R , the series network is halted. Consequently, the current iteration is considered unfit for pattern recognition and hence, test results from the previous iteration are taken into account as the final network prediction.

The R value can be selected based on rejection trends observed in past results from similar neural

network tests for known output parameters. However, if this history is not available, then Equation 3 can be applied, where K is the number of trials or samples required. This expression is considered valid since for R exceeding K , the bulk of the sample distribution no longer supports the trained network for pattern recognition.

$$R \leq K \tag{3}$$

4 Pattern Recognition for a Guided Waves Application

The pattern recognition system implementing the WRS technique and the ISR criterion was integrated into a damage identification tool for a guided waves application. The application selected was the identification of thin damages in beams, which are elementary members in frames and trusses for many civil and aerospace structures.

Test patterns were obtained from measurements of the transient wave responses on beams fabricated with artificial damages. On the other hand, training patterns were generated from a simulation that was based on the fundamental principles of wave propagation, reflection and transmission. Both patterns were preprocessed using the discrete wavelet transform, improving correspondence between experimental and simulated patterns while reducing the neural network processing time.

A feedforward backpropagation neural network architecture was selected for the pattern recognition system. Neural network parameters like the hidden number of neurons and the training set size were then designed to optimize the damage identification performance.

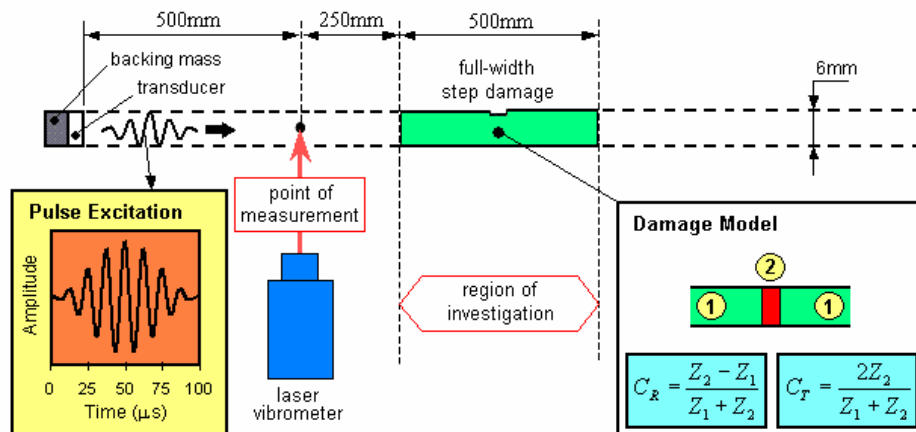


Fig. 2 Beam specimen with a fabricated full-width step damage, illustrating the point of measurement and the region of investigation. Pulse Excitation inset shows the 8-cycle 80kHz Hanning windowed tone burst pulse as the interrogating wave while the Damage Model inset shows the inhomogeneity model for simulating training patterns.

4.1 Experiment

Aluminium beam specimens of 2 metres in length with rectangular cross-sections 12mm × 6mm were considered, as depicted in Figure 2. A longitudinal Pz27 piezoceramic transducer was adhesively bonded to one end of the beam to excite an interrogating wave pulse. The transducer was wired to a function generator to produce an 8-cycle 80kHz Hanning windowed tone burst pulse excitation. An amplifier was connected between the function generator and the transducer to increase the amplitude of the signal. Additionally, for a better signal-to-noise ratio response, a brass backing mass was bonded to the transducer with epoxy adhesive. A Polytec OFV 303/OFV 3001 laser vibrometer system [2] was used to measure the transient wave response at the centre of the 6mm thickness surface of the beam. Measurements were collected at 500mm from the transducer end to ensure that there was minimum pulse interference in the signal. Out-of-plane displacement was measured against time, which was displayed on a digital oscilloscope and saved on a personal computer.

On each beam, a full-width step damage was machined in a region of investigation located at the centre of the beam. This 500mm long region was taken as the original damage parameter space. Three beams with fabricated damages, labeled as T1, T2 and T3, were prepared for experiments. The three full-width step damages are described in Table 1. As tabulated, three damage parameters would be identified by pattern recognition. Note that DCP was measured from the transducer end.

| | Damage Centre Position, DCP (mm) | Damage Depth, DD (mm) | Damage Length, DL (mm) |
|---------|----------------------------------|-----------------------|------------------------|
| Beam T1 | 960 | 1.1 | 90.1 |
| Beam T2 | 1000 | 1.0 | 40.1 |
| Beam T3 | 1100 | 1.9 | 75.0 |

Table 1 Damage parameters fabricated on 3 test beams.

4.2 Simulation

The arrival times of wave pulses at the point of measurement were approximated from the longitudinal wave velocity, c , which was measured to travel at 4750m/s. At the damage region, the wave was split into reflected and transmitted waves [12]. To quantify the proportion of reflection and transmission, the damage region was modeled as an inhomogeneity [5], as shown in the Damage Model

inset in Figure 2. The inhomogeneity was the same in length as the damage but had different acoustic wave impedance, Z , compared to the aluminium beam. Z is a material property, as defined in Equation 4 where ρ is the material density, c is the wave velocity, and A is the cross-sectional area.

$$Z = \rho c A \tag{4}$$

For the step damage, there was a change in Z due to a change in A , which was a function of the beam thickness. Reflection and transmission coefficients at the boundaries of the damage region, C_R and C_T respectively, can thus be derived from Equation 5.

$$C_R = \frac{Z_2 - Z_1}{Z_1 + Z_2}, C_T = \frac{2Z_2}{Z_1 + Z_2} \tag{5}$$

With c , C_R and C_T known, signals of the transient wave response at the point of measurement for different damage parameters could then be generated by simulation. The parameter space and the level of accuracy for the damage parameters are shown in Table 2. Training data was simulated within these parameter spaces and accuracies.

| | Parameter Space (mm) | Accuracy Level (mm) |
|-----|----------------------|---------------------|
| DCP | 750 - 1250 | 1 |
| DD | 0 - 3.0 | 0.1 |
| DL | 0 - 100.0 | 0.1 |

Table 2 Damage parameter properties for simulation.

4.3 Experimental and Simulated Signals

The transient wave response signals captured on the oscilloscope at the point of measurement for the three test beams are given in Figures 3(a). Low noise levels were achieved in the experimental signals, thus the laser vibrometer was concluded to be an excellent measuring instrument for guided waves. The equivalent signals simulated are also plotted in the corresponding figures. Both signals were normalized by the amplitude of the incident wave. A reasonably good match with respect to pulse amplitudes and pulse arrival times was observed between experimental and simulated signals for all three test beams.

Signals in the 100µs-940µs range had been selected as neural network input patterns because this period was rich with information regarding the damage. Wave response beyond this range was not

considered due to the presence of severe attenuation and dispersion [12], which were features not included in the simulation. The range spanned from the incident wave to the first transmitted wave. The first transmitted wave was defined for a pulse that had traveled past the damage, reflected from the free end of the beam, and transmitted again through the damage before being collected at the point of measurement.

Four main pulses can be observed in all three experimental or simulated signals. The first and last large amplitude pulses are the incident and first transmitted waves respectively. The two other pulses in between are the first reflected wave from the damage followed by its reflection from the beam transducer end.

The first reflected wave for T1 had a different waveform because the length of its damage was long enough to cause a clear separation between the waves reflected from the two ends of the damage. For T3, a fifth pulse was observed at the end of the signal, interfering the first transmitted wave. This

pulse was the second reflection of the first reflected wave from the damage. The arrival times of all the pulses could be easily checked from simple calculations with the known wave velocity and the distance traveled along the beam.

Although the arrival times and pulse amplitudes matched reasonably well between experimental and simulated signals, there were substantial differences in the phase. The discrepancies in the phase were attributed to complex dispersive behaviours of waves propagating in rectangular beams [13]. These properties could only be approximated with limited accuracies through elaborate numerical methods [14] and hence, were not included in the simulation.

Another feature not found in the simulated signal was a small tailing pulse after the incident wave, which was present in the experimental signals of T1 and T3. The additional pulse was the result of a flexural mode excited at the transducer-beam interface. Since the presence and magnitude of this flexural mode was random, this effect was also excluded in the simulation.

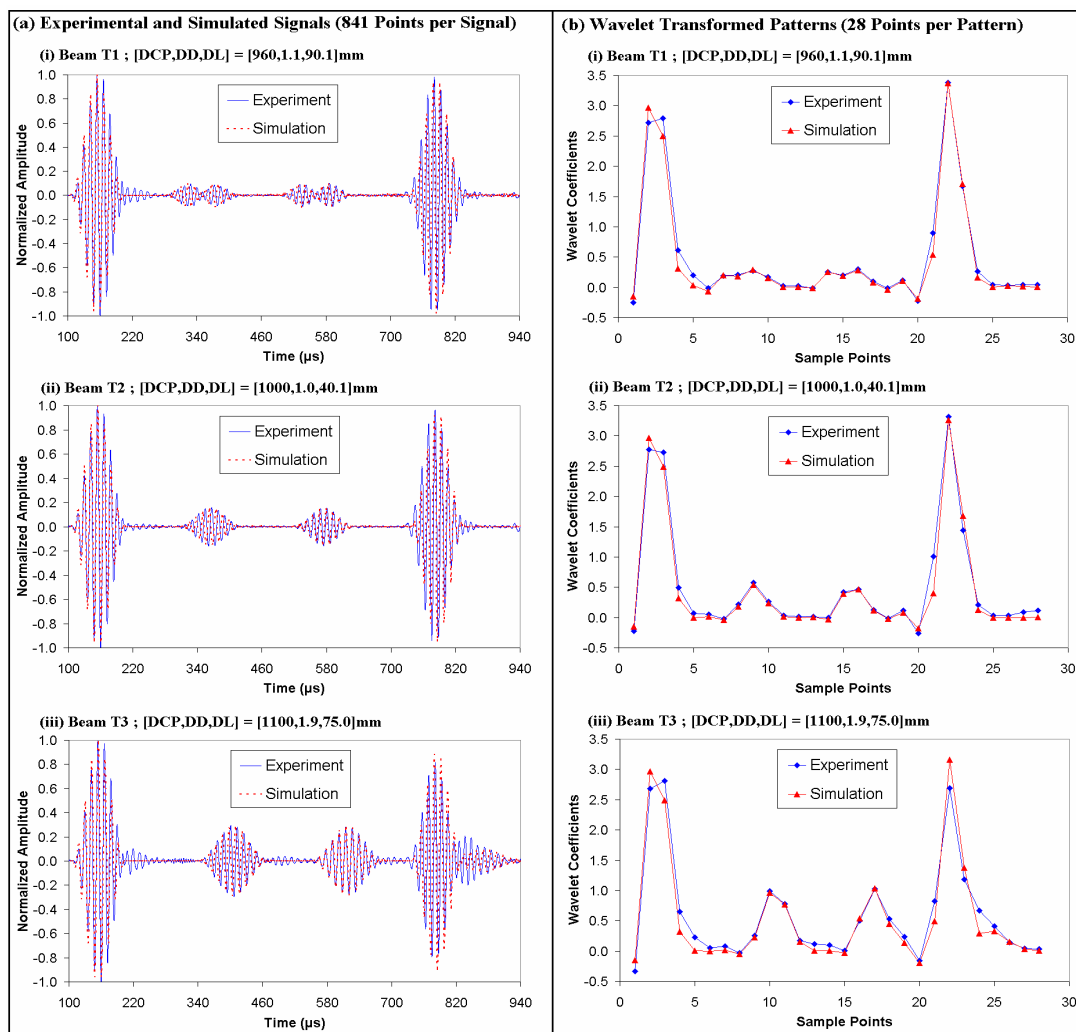


Fig. 3 Experimental and simulated signals with corresponding preprocessed wavelet patterns for the three test beams.

4.4 Wavelet Transform Preprocessing

Discrepancies in the phase and the presence of the flexural mode could lead to errors in pattern recognition. Hence, preprocessing was proposed to minimize these effects and to extract only important features from the signals. The discrete wavelet transform was applied, which decomposed the signal by reducing the number of sampling points through a wavelet derived filter bank in dyadic scales [3].

The absolute signals were transformed to produce wavelet patterns, as shown in Figure 3(b). These wavelet patterns were the result of 5 levels of decomposition with the 8th order Daubechies wavelet. Essential features that described the damage like the pulse arrival times, magnitudes and widths, were preserved in the wavelet patterns.

The number of points in the pattern was also reduced from 841 points at a sampling rate of 1MHz to 28 points. The shorter wavelet pattern thus provided an additional advantage in faster processing times when learning the simulated patterns during neural network training.

4.5 Neural Network Architecture and Design

The multi-layer perceptron with a single hidden layer of neurons [7] was the selected neural network architecture for pattern recognition. This neural network contained a hyperbolic sigmoid activation function, F , to account for nonlinear regression. The governing function is given in Equation 6 where I is the input, O is the output, M is the total neurons, W is the weight, and B is the bias. $U = 28$ for the total points in the input pattern while $v = 1, 2$ or 3 for the three damage parameters identified.

$$O_v = \sum_{m=1}^M W_{v,m} F \left(\sum_{u=1}^U W_{m,u} I_u + B_m \right) + B_v \quad (6)$$

Training was supervised with weights and biases adjusted via a resilient backpropagation algorithm [15] by minimizing the mean square error between outputs and targets. The three damage parameters were scaled in the range $[-1, 1]$ for training due to the difference in orders of magnitude. Validation with early stopping [7] was applied during training to improve generalization. The size of the validation set was taken as half that of the training set.

A systematic approach [16] was adopted to design the optimum number of neurons in the hidden layer and the size of the training set. The designed parameters are summarized in Table 3. The same architecture and design was maintained throughout the series network for consistency assuming that a network that worked well for a

training range would work equally well for a subset of the range.

| Number of Neurons | Training Set Size | Validation Set Size | Network |
|-------------------|-------------------|---------------------|---------|
| 10 | 4845 | 2423 | 28-10-3 |

Table 3 The designed neural network parameters.

5 Results and Discussion

28-10-3 neural networks were formed in a series and were run in MATLAB® for all three test cases, based on WRS described in Figure 1. $I_{max} = 3$ because beyond this, there would be a high chance for the actual damage parameters to fall outside the training range, especially for DD and DL with small original parameter spaces. $K = 50$ was selected to obtain an adequate number of samples to represent the distribution of the results while $R = 50$ provided the maximum allowance in rejections, according to Equation 3. Test results from each iteration are shown and discussed in the following subsections.

5.1 Potential of the WRS Technique

An example of errors from 50 samples collected in I_0 for the same training set is shown in Figure 4. For comparison, errors from both the experimental and the equivalent simulated test patterns for the same initial weights as per sample were plotted. Although test patterns matched reasonably well, as seen in Figure 3(b), there was significant difference in pattern recognition results. The mean from the experimental samples, referred as the Average Bias, also reported worse results compared to simulation.

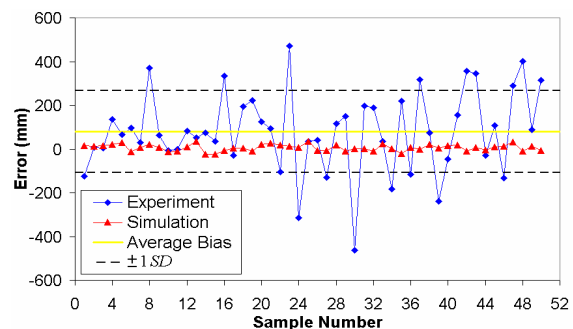


Fig. 4 Sample error results for DCP of T3 in I_0 .

There were many experimental samples that yielded predictions equal or better in quality compared to simulation, for example in sample numbers 2, 3, 7, 10, 11, 17, 25, 33 and 44, which constituted 18% of the total samples. On the other hand, there were 21 or 42% of the samples that had errors less than 100mm or 10% of the original DCP

parameter space size. Summarized results for other damage parameters and test beams are provided in Table 4. The table shows that the number of quality samples was quite consistent across the test beams for each damage parameter. However, the numbers dropped by around 50% from DCP to DD to DL. This indicated the order in the level of difficulty in recognizing these parameters, which was dependent on the quality of the mapping between pattern inputs and the respective damage parameters. Overall, these observations showed the essence of selecting initial network weights for more accurate results.

| | No. of samples (% of total samples) | | |
|---------|-------------------------------------|----------|---------|
| | DCP | DD | DL |
| Beam T1 | 20 (40%) | 11 (22%) | 5 (10%) |
| Beam T2 | 22 (44%) | 11 (22%) | 5 (10%) |
| Beam T3 | 21 (42%) | 9 (18%) | 7 (14%) |

Table 4 Observed quality samples during I_0 with errors below 10% the damage parameter space size.

The actual damage parameters were observed to be within the $\pm 1 \sigma$ of the experimental sample results. This was also found to be true for other damage parameters and test beams. Hence, from Equation 1, $n = 1$ was selected to allow training range reduction for subsequent neural network processing for improved generalization with WRS.

5.2 Performance of the WRS Technique with the ISR Criterion

The damage identification results for the individual iterations are plotted as histograms in Figure 5. The series network was deliberately run up to $I_{max} = 3$ even if R was exceeded to examine the functionality of the ISR criterion. The arrows in the figure point to results that were selected based on ISR. Percentages shown refer to the improvement in results selected when compared to results from I_0 , which were then normalized by the respective original parameter space or training range sizes from Table 2. The formula to calculate the percentage is given in Equation 7 where the terms e_0 and e_{ISR} are the absolute average biases from I_0 and from the ISR selected output respectively.

$$\text{Improvement with WRS + ISR} = \frac{e_0 - e_{ISR}}{UL_0 - LL_0} * 100\% \quad (7)$$

The accuracy of the results generally fluctuated among the iterations. This was due to prediction tolerance common in neural networks [7], mainly caused by changes in the training patterns and

random initial weights, which are part of the processes in the series network. The tolerance level was relatively high for DD of T1 due to the difficulty in recognizing this parameter from the small reflected pulse amplitudes in the pattern that described the damage, as seen in Figure 3(i).

The WRS technique only provided benefit for test cases where the damage was poorly recognized initially, as evident in DCP and DD of T3, and in DL of T1 and T2. DCP of T3 achieved the best improvement at around 14%. Once the identified parameter was within the tolerance range of its best perceived prediction, significant improvements would not be achieved in subsequent iterations but instead, fluctuations would result and potentially worse results could be obtained like in DD of T1.

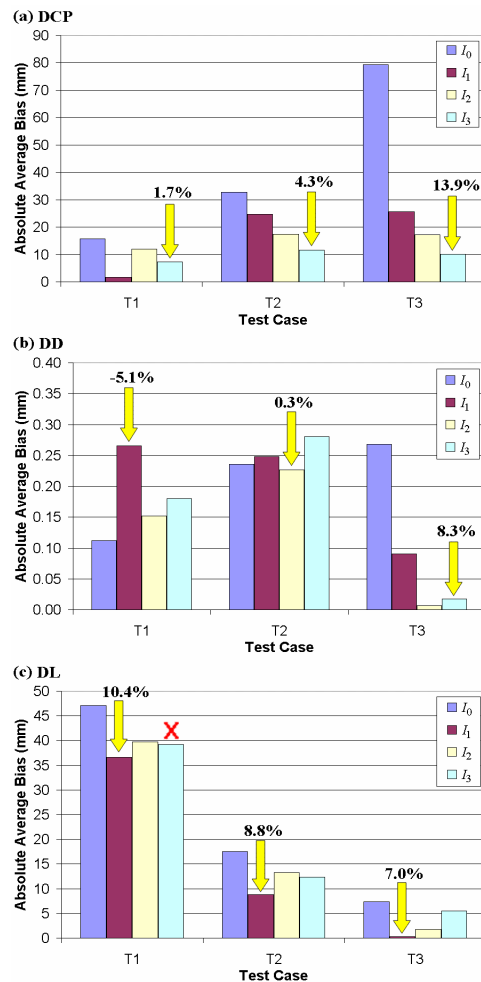


Fig. 5 Damage identification results for a series network applied with the WRS technique and the ISR criterion.

The main objective of the ISR criterion was to select a result before the actual damage parameter fell outside of the training range, as marked by a cross in Figure 5. Only one such case was observed, DL of T1, where the criterion had performed well to select a result before extrapolation was required for

pattern recognition. For DD and DL, the majority of the selections were made before I_{\max} , indicating high rejections in early iterations. This was caused by small original training ranges and the difficulty in identifying these parameters from the patterns, yielding possibly large tolerances. Further iterations could be run for test cases where R had not been exceeded but more likely than not, these cases had already arrived within the tolerance range of the best perceived predictions. Negative improvement was obtained for DD of T1 based on ISR but this cannot constitute a failure of the criterion because the aim of ISR was not to pick the most accurate prediction among iterations. However, the ability for ISR to select the best results among the iterations for more than half the test cases suggested that there might be a correlation between R and prediction accuracy, which requires further investigations.

6 Conclusion

Test pattern dependency in WRS is an interesting concept that shows promising potentials for improving the performance of regression neural networks. This method is specifically designed for pattern recognition problems that contain relatively high uncertainties in predictions among samples with random initial weights. One practical example of an application is damage identification in beams using guided waves with simulated training patterns and experimental test patterns where WRS trained series network and ISR selected results could yield up to 14% improvement in prediction accuracies.

The WRS technique is also a flexible module that can complement other training methods, for example in bagging or boosting. The technique also encourages further development to improve its effectiveness in retrieving the most accurate predictions. Statistical analysis of the samples to determine the limits for parameter space reduction, output results selection criterion, and correlation between ISR and prediction accuracy are examples of possible areas for further studies.

7 Acknowledgements

C.K. Liew is grateful for the support received from an International Postgraduate Research Scholarship (IPRS) awarded by the Australian Department of Education Science and Training (DEST), and a UQ Graduate School Scholarship (UQGSS) awarded by the University of Queensland (UQ). The authors would also like to thank Assoc. Prof. David Mee for his advice from a few invaluable discussions.

References:

- [1] W.J. Staszewski, C. Boller and G.R. Tomlinson, *Health Monitoring of Aerospace Structures*, John Wiley & Sons Ltd., 2004.
- [2] M. Staudenmann, *Structural Waves in Nondestructive Testing*, Institute of Mechanics, Swiss Federal Institute of Technology, 1995.
- [3] C.K. Liew and M. Veidt, Evaluation of Laminar Defects in Beams using Guided Waves and Pattern Recognition Techniques, *Proceedings of the 1st International Conf. on Structural Condition Assessment, Monitoring and Improvement*, 2005, pp. 231-238.
- [4] Z. Su and Y. Lin, An Intelligent Signal Processing and Pattern Recognition Technique for Defect Identification using an Active Sensor Network, *Smart Materials and Structures*, Vol.13, 2004, pp. 957-969.
- [5] C.H. Wang and L.R.F. Rose, Wave Reflection and Transmission in Beams Containing Delamination and Inhomogeneity, *J. Sound and Vibration*, Vol. 264, 2003, pp. 851-872.
- [6] C. Yang, L. Ye, Z. Su and M. Bannister, Some Aspects of Numerical Simulation for Lamb Wave Propagation in Composite Laminates, *Comp. Struct.*, Vol. 75, 2006, pp. 267-275.
- [7] C.M. Bishop, *Neural Networks for Pattern Recognition*, Oxford University Press, 1995.
- [8] A. Zaknich, *Neural Networks for Intelligent Signal Processing*, World Scientific, 2003.
- [9] A.J.C. Sharkey, *Combining Artificial Neural Nets: Ensemble and Modular Multi-Net Systems*, Springer-Verlag, 1999.
- [10] E. Barnard and L.F.A. Wessels, Extrapolation and Interpolation in Neural Network Classifiers, *IEEE Control Systems Magazine*, Vol. 12, No. 5, 1992, pp. 50-53.
- [11] C. Moler, 10^{435} is a Very Long Time, *MATLAB News and Notes*, Fall Issue, 1995, pp. 12-13.
- [12] K.F. Graff, *Wave Motion in Elastic Solids*, Dover Publication Inc., 1991.
- [13] M.A. Meddick, On Dispersion of Longitudinal Waves in Rectangular Bars, *Journal of Applied Mechanics*, Vol. 34, 1967, pp. 714-717.
- [14] W.B. Fraser, Stress Wave Propagation in Rectangular Bars, *International Journal of Solids Structures*, Vol. 5, 1969, pp. 379-397.
- [15] H. Demuth and M. Beale, *Neural Network Toolbox User's Guide*, MathWorks Inc., 2004.
- [16] C.K. Liew and M. Veidt, Optimization of Neural Network Pattern Recognition Systems for Guided Waves Damage Identification in Beams, *Proceedings of the 33rd Annual Review in Quantitative Non-Destructive Testing*, 2006.